Measurements of scattering by suspensions of irregularly shaped sand particles and comparison with a single parameter modified sphere model

Peter D. Thorne[a)]
Proudman Oceanographic Laboratory, Joseph Proudman building, 6 Brownlow Street, Liverpool L3 5DA, United Kingdom

Michael J. Buckingham
Marine Physical Laboratory, Scripps Institution of Oceanography, University of California, San Diego, 9500 Gilman Drive, La Jolla, California 92093-0238

(Received 12 August 2003; revised 4 August 2004; accepted 30 August 2004)

Measurements are presented of multi-frequency underwater acoustic backscattering from suspensions of glass spheres and sands. The data were collected in a sediment tower, specifically designed for such measurements and capable of generating a homogeneous suspension over a distance of approximately 1 m. The glass sphere data were collected to assess the capability of the system and for calibration. The measurements on suspensions of sands were obtained as part of on-going studies into the measurement of nearbed sediment transport processes using acoustics. Utilizing the backscattered sound from sand suspensions, both the form function and total scattering cross section of the sediments have been measured for a range of sediments and particle sizes. Interpretation of the observations has been carried out within a framework of sphere scattering. The results show enhanced scattering for suspensions of sand grains, relative to that of similar size spherical scatterers and the enhancement can be described by a function dependent on the particle size and the wave number of the insonifying sound, with one free parameter. © *2004 Acoustical Society of America.* [DOI: 10.1121/1.1808458]

PACS numbers: 43.30.Ft, 43.30.Gv, 43.30.Pc [KGF] Pages: 2876–2889

I. INTRODUCTION

The development of our understanding of sediment transport processes, over sandy beds, has benefitted greatly from recent developments in the application of acoustics to this problem.[1] The potential of acoustics to provide co-located, simultaneous measurements of the seabed morphology, the sediment field, and the hydrodynamics, provides opportunities to examine how these three mutually interactive and interdependent components interrelate with each other. The idea of using acoustics for such studies is attractive and straightforward. A pulse of high frequency directional sound, typically in the range 0.5–5 MHz and centimetric in length, is transmitted from a source usually mounted around a metre above the bed. As the pulse propagates down towards the bed, sediment in suspension backscatters a proportion of the sound and the bed generally returns a strong echo. This signal has the potential to provide information on profiles of suspended sediment parameters, the flow, and the time history of the bedforms. The aim of such measurements is to provide sedimentologists and coastal engineers with new measuring capabilities for studying sediment entrainment and transport.

In the present study the focus is on the measurement and description of the scattering characteristics of suspensions of glass spheres and sands. The backscattering characteristics are formulated in terms of the form function and the attenuation through the total scattering cross section. These descriptions are at the kernel of the inversion to extract the suspended sediment component from the backscattered signal. Also, generically, although the scattering properties of a number of canonically shaped bodies are reasonably well understood, there are many natural scatterers that are irregular in shape and a description of such bodies is required. To date the data published on the backscattering characteristics of suspensions of irregularly shaped sand particles have been limited to the works of Hay.[2,3] These works form the basis of our current description of the backscattering properties of suspensions of marine sands. A further work has supported this general description.[4] However, a more recent detailed study on the attenuation characteristics[5] of sand suspensions showed significantly higher attenuation values than predicted by the commonly employed sphere-based scattering models[6] and somewhat larger than may have been anticipated on the basis of the previous scattering measurements.[2,3,7] This result led the present authors to revisit the form function and total scattering cross section characteristics for suspensions of sand and to this end a series of measurements were collected on different sand samples to examine their scattering properties. With the exception of one reported data set,[2] the measurements on the scattering properties of sediments have either measured the form function or the total scattering cross section; however, in the present study, both scattering prop-

[a)]Current address: Proudman Oceanographic Laboratory, Joseph Proudman Building, 6 Brownlow Liverpool L3 5DA, United Kingdom. Electronic mail: pdt@pol.ac.uk

erties were measured from the backscattered signal. The ability to measure both scattering parameters simultaneously provided an opportunity to assess the consistency of the descriptions of the form function and the total scattering cross section.

To provide a description of the scattering properties of the irregularly shaped sand sediments, calculations based on a simple analytical shape, the sphere, have been used. This approach of using canonically shaped representations with analytical solutions is common and has been used for both sediment[2–8] and biological scatterers.[9–11] The results from this study show both the form function and total scattering cross section can be reasonably well represented by a quartz sphere model, modified by an enhanced scattering function, dependent on the suspension particle "radius," a_s, and the wave number, k, of the sound in water, with one free parameter. The word radius is placed in quotation marks to indicate the definition of particle radius has a degree of ambiguity for irregularly shaped particles and this is considered later. The justification for using an enhancement factor which is dependent on ka_s is based on two premises. The first is that, in the Rayleigh region,[12] $ka_s \ll 1$, scattering is considered to be independent of the shape of the scatter. Though this is only strictly true for a fluid scatterer, one might anticipate elastic spherical and irregularly shaped scatterers may have similar scattering characteristics.[13] For $ka_s \gg 1$, sometimes known as the geometric regime, there is a theorem that states the geometric cross section of a convex particle, averaged over all orientations, is equal to a quarter of the surface area of the particle.[14,15] Given that a sphere has the minimum surface area to volume, then a particle of irregular shape, having a similar volume to a sphere, would have a larger surface area and hence a higher geometric and scattering cross section. This, therefore, leads straightforwardly to the expectation that there will be a functional dependence on ka_s of the scattering characteristic of a suspension of sand, relative to spheres having the same volume, and, as will be shown later, this approach requires only one free parameter to account for the difference between sphere and sand grain scattering. This methodology differs from that of Ref. 5 which used a two parameter equivalent sphere model. Two parameters were required to fit their observations to a sphere model because the functional dependence on ka_s, of irregularly shaped particle scattering relative to a sphere, was not considered. It will be shown here that the data in Ref. 5 can be represented by the approach adopted in the present paper.

II. SUSPENSION SCATTERING

For incoherent scattering, when the scattered phase is random and uniformly distributed over 2π, the recorded root-mean-square backscattered voltage, V, from a suspension of sediments, insonified with a piston source transducer, can be written[1,2,6,8] as

$$V = \frac{K_s K_t M^{1/2}}{r\psi} e^{-2r\alpha},$$

$$K_s = \frac{f_m}{(\rho\langle a_s\rangle)^{1/2}}, \quad K_t = P_o r_o \Re T_v \left\{\frac{3c\tau}{16}\right\}^{1/2} \frac{0.96}{ka_t}, \tag{1}$$

$$\alpha = \alpha_\omega + \frac{3}{4\rho_s r}\int_o^r \frac{\chi_m}{\langle a_s\rangle} M\, dr.$$

The term K_s represents the sediment backscattering properties, ρ_s is the sediment grain density, $\langle a_s\rangle$ is the mean particle radius of the sediment in suspension and $f_m = \{\langle a_s\rangle\langle a_s^2 f^2\rangle/\langle a_s^3\rangle\}^{1/2}$, where f is the form function in the backscatter direction and describes the backscattering characteristics of the scatterers. $\chi_m = \{\langle a_s\rangle\langle a_s^2\rangle\chi/\langle a_s^3\rangle\}$, χ is known as the total scattering cross section and describes the scattering attenuation characteristics of the scatterers. $\langle\ \rangle$ represents an average over the particle size distribution of the sediments in suspension. The term α_ω is the sound attenuation due to water absorption, M is the concentration of sediment in suspension, r is the range from the transducer, and ψ accounts for the departure from spherical spreading within the transducer nearfield.[16] For fixed settings K_t is a system constant. This comprises of the reference pressure, P_o, normally defined at $r_o = 1$ m, $\Re$ is the receive sensitivity, T_v is the voltage transfer function for the system, $c\tau$ is the pulse length, where τ is the pulse duration and c is the velocity of sound in water, k is the wavenumber of the sound in water, and a_t is the radius of the transducer.

To evaluate Eq. (1) the magnitude of the backscatter form function and the total scattering cross section are required. For a sphere these can be expressed[8,17] as

$$f = \left|\frac{2}{ix}\sum_{n=0}^{n=\infty}(-1)^n(2n+1)b_n\right|, \tag{2a}$$

$$\chi = \left|\frac{-2}{x^2}\sum_{n=0}^{n=\infty}(2n+1)\mathrm{Re}(b_n)\right|, \tag{2b}$$

where b_n is a function of spherical Bessel and Hankel functions of the first kind and their derivatives, Re denotes taking the real part of the complex expression, and $x = ka$, where a is the radius of the sphere. For the scattering of suspensions of sand a definition is required for the particle size and, from the discussion at the end of the Introduction, ascribing an equivalent sphere dimension is not readily defined. Even if one were to adopt the radius of a sphere with the equivalent surface area to that of the grains, obtaining such measurements for a suspension of sand grains would seem problematic. Therefore a pragmatic approach was taken and the size measured by sieving the sediments into relatively narrow size fractions was taken to define the particle size. Such an approach is not arbitrary, since most sedimentologists use sieving to define the particle size of sands and the end product of the application of acoustics to sediment processes is to deliver to the sedimentologist measurements of parameters they can readily utilize. In the present study the experimental expressions for the scattering parameters were

chosen to be independent of particle size. Taking the natural logarithm of Eq. (1), we can write for a homogenous suspension (as was the case in the present study, see Figs. 3 and 4)

$$\ln(Vr\psi)=\ln\left(f_m K_t\sqrt{\frac{M}{\rho_s\langle a_s\rangle}}\right)-2r\left(\alpha_w+\frac{3\chi_m M}{4\rho_s\langle a_s\rangle}\right). \tag{3}$$

This is now a simple linear equation in $\ln(Vr\psi)$ and r, and allows the following to be written

$$f_x=\frac{e^{\eta}}{K_t}\sqrt{\frac{\rho_s}{kM}}, \tag{4a}$$

$$\chi_x=\frac{2\rho_s}{3kM}(\kappa-2\alpha_w), \tag{4b}$$

where η and κ are respectively the intercept and the magnitude of the gradient obtained from the measurements as expressed in Eq. (3). Here we have used $f_x=f_m/\sqrt{x}$ and $\chi_x=\chi_m/x$, and for the measured values $x=k\langle a_s\rangle$ and $\langle a_s\rangle$ was the sieved sediment radius. The advantage of this form of expression is the rhs of Eqs. (4a) and (4b) do not depend on a definition of particle size.

To compare a sphere based scattering model with the measurements collected on suspensions of sands a simple modification to Eq. (2) was applied for consistency with the experimental definitions of f_x and χ_x. These equations are now written as

$$f_s=\gamma\langle f/\sqrt{x}\rangle, \tag{5a}$$

$$\chi_s=\gamma\langle\chi/x\rangle, \tag{5b}$$

where $\langle\ \rangle$ represents an average over a range of x. This essentially operates as a low pass filter and reduces the variation in f_s and χ_s associated with the acoustic resonances of a sphere (see Refs. 1–6). γ is the function in Eq. (5) which will be used to account for the difference in the scattering level, with x, between the low pass sphere model [i.e., Eq. (5) with $\gamma=1$] and the measured values for suspensions of sand, obtained from Eq. (4).

III. SEDIMENTS USED IN THE STUDY

A series of measurements was taken on glass spheres and seven different sands collected from estuarine, beach, and quarried locations. In Fig. 1 are scanning electron micrographs of the sediments used. The sand sediments labelling of (a) to (g) is consistent and is used in Fig. 1, Table I and Figs. 9 and 10. The glass spheres can be seen to be nominally spherical in shape, although it can be readily observed there was some departure from perfect sphericity. Although the glass sediments were not ideally spherical, studies on such suspensions[2,5,8,18] have shown their scattering characteristics are well represented by the theoretical description of a sphere. For the sphere calculations of the form function and total scattering cross section, the material properties chosen were based on measurements.[19] The values used for the compressional and shear wave velocities were respectively 5550 and 3545 ms^{-1}, with a density of 2500 $\mathrm{kg\,m}^{-3}$. For water the values used for density and sound velocity were 1000 $\mathrm{kg\,m}^{-3}$ and 1480 ms^{-1}. The comparison of the glass sphere prediction and measured form function is not highly sensitive to the sphere velocities chosen, within approximately $\pm5\%$ of the above values, since they primarily control the resonance structure of the form function and, as will be seen later, these are only weakly observed when there is even a small departure from a uniform particle size in suspension.

The seven scanning electron micrographs of the sediments show in detail the size and shape of the sediments used in the study. None of the particles are particularly spherical; in fact, it would be difficult to formulate a geometric shape which accurately represents the profiles of the particles. Generically they could be described as irregular in form, with curved surfaces, facets, and edges. It does appear that some sediments are more rounded than others, for example, sample "*a*" sediments look as if they are somewhat smoother than the sediments "*b*," which appear more angular. Also sediment "*f*" has some particle shapes which were relatively flat in form. The effect these changes in particle shape have on the acoustic scattering properties of suspended sediments will influence whether or not a general description of the form function and total scattering cross-section can be obtained, which has wide-ranging applicability. All the sediments studied were sand grains, primarily composed of quartz and, for the calculations to follow, the density, compressional, and shear wave velocities were taken[20] to be respectively 2650 $\mathrm{kg\,m}^{-3}$, 5980 ms^{-1}, and 3760 ms^{-1}. Again the choice of velocities was not critical because variations of up to $\pm10\%$ did not significantly alter the modified low pass sphere solution given by Eq. (5).

To study both the suspensions of glass spheres and sand grains, the sediments were sieved into $\frac{1}{4}\ \varphi$ ($\phi=-\log_2 d$ where d is the particle diameter in millimeters) narrow size fractions. Table I shows the values of $\langle a_s\rangle$ for the sediments studied and the number of experiments conducted on each sediment and each size fraction.

IV. DESCRIPTION OF THE SEDIMENT TOWER

The experimental arrangement used to measure the scattering properties of glass sphere and sand suspensions is shown in Fig. 2. The sediment tower was constructed from Perspex, with the main component being a vertical 2.15 m tube, with an inner diameter of 0.3 m and wall thickness of 0.01 m. Once the tower was filled with a suspension, bilge pumps were used to extract water and sediment from the bottom of the tower and deliver it back to the top of the tower through a 0.05-m-diam pipe. Two bilge pumps, pumping side by side, operating at approximately 50% of their maximum capacity, were chosen for this function. Operating in this mode prevented pump cavitation and thereby reduced the possibility of introducing air into the system through the pumping mechanism. Also two pumps generated sufficient flow in the return pipe to ensure the sediments extracted with the water from the bottom of the tower were returned to the top. At the top of the tower the suspension was reintroduced below the upper water surface, open to the atmosphere, through a mixing chamber, designed to homogenize the suspended sediments within the tower, without the entrainment of air. Further to assist with the homogeneity of the suspension, a unit near the base of the tower, consisting of a turbu-

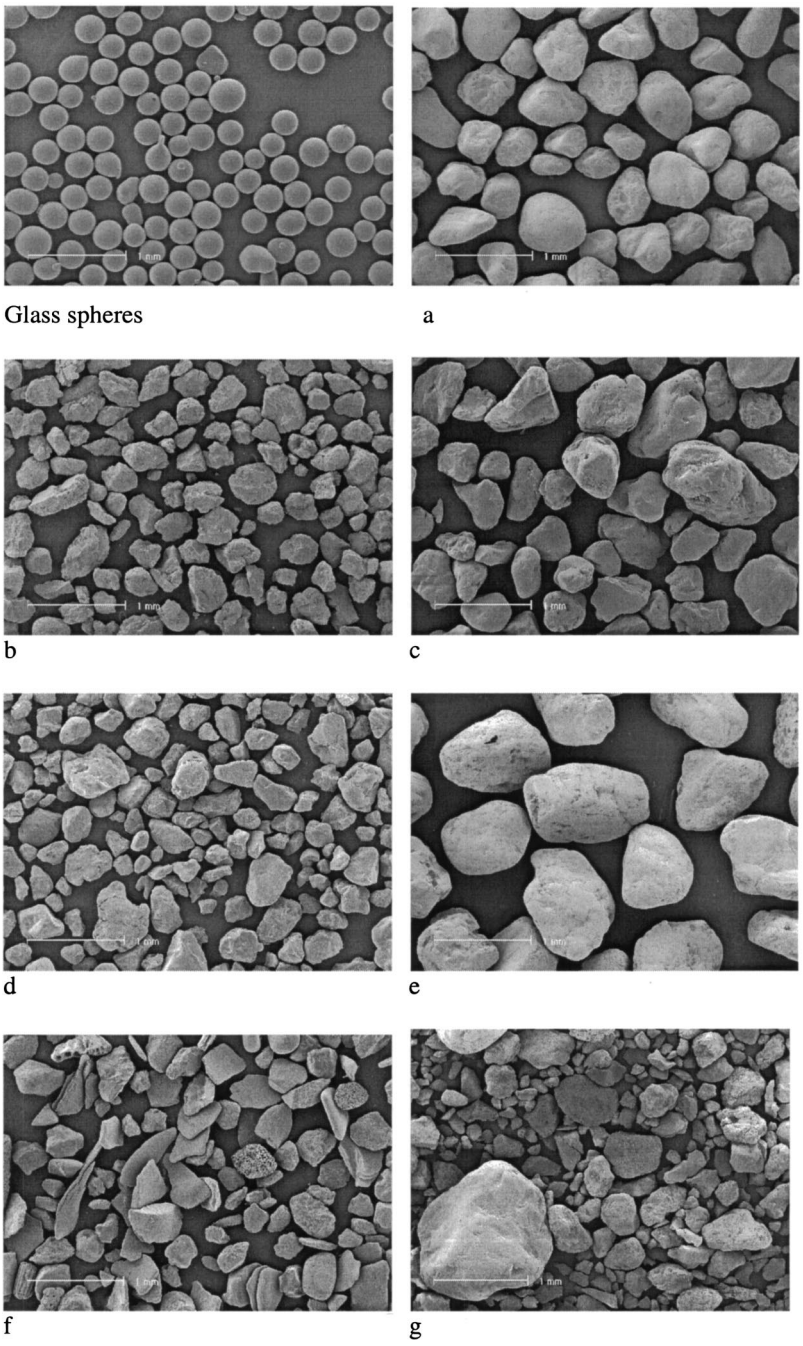

FIG. 1. Scanning electron micrographs of the glass spheres and sands used in the study.

lence grid, impeller, and propeller, was rotated to generate an upward mixing turbulent flow. This combination of mixing elements was designed to generate a uniform suspension throughout the tower.

To assess the homogeneity of the suspension in the tower three experiments were conducted using suspensions. The sediments used were glass spheres with $\langle a_s \rangle = 115.5\,\mu$m and $\langle a_s \rangle = 195\,\mu$m, and sand with $\langle a_s \rangle = 195\,\mu$m. Pumped samples of the sediments were collected between 0.1 and 0.8 m below the transducers, and located on the central vertical axis of the tower, at 0.07 m from the axis, and at 0.14 m from the axis; the latter was within 0.01 m of the tower wall. Know volumes of water were extracted, passed through a filter, and the retained sediments dried and weighed. The concentration was then calculated as the dried mass divided by the volume of water extracted. The resultant measured concentrations are given in Fig. 3. The data clearly show the suspended sediments were homogeneous both across the tower and vertically. There was no significant difference with sediment size or between the glass spheres and the sand. These measurements clearly show the sediments in suspension were homogeneous and uniform with range below the transducers.

To obtain the scattering measurements a triple frequency acoustic backscatter system operating at 1.0, 2.0, and 4 MHz was mounted in the upper section of the tower. The transducers had respective nominal −3-dB half beamwidths of 3.1°, 2°, and 1.2°. The system measured the envelope of the backscattered signal at 0.01-m intervals over a range of 1.28 m. For data collection a low pulse repetition frequency of 4 Hz was used to allow the sound from one transmission to dissipate before the following transmission. For each measure-

TABLE I. The table shows the number of experiments conducted, at each sediment size, for the different sediments. The total column and row respectively give the number of experiments conducted on each sediment and for each size. β_f and β_χ respectively give the values for β in Eq. (7) for calculating f_s and χ_s.

$\langle a_s \rangle$ (μm)	Glass	a	b	c	d	e	f	g	Total
45.0								2	2
57.75	3				2		7	2	11
68.75	3				2		3	2	7
82.5	3		3	1	2	3	5	4	18
98.0	5			2	1	1	3	2	9
115.5	16		1	2	1	1	4	2	11
137.5	11		2	3		1	3	4	13
163.75	2	5		4		1	5	2	17
195.0	9	5	1	3		1	6	6	22
231.25	5	8		3		1	5	4	21
275.0	3	5		5					10
327.5	3	3		4		2			9
390	3			1					1
Total	66	26	7	28	8	11	41	30	151
β_f		2.1	1.7	2.4	1.6	2.0	2.4	1.4	1.9±0.4
$\sigma(\beta_f)$		0.4	0.3	0.5	0.2	0.2	0.3	0.2	
β_χ		1.6	1.9	1.8	1.7	1.8	1.7	1.4	1.7±0.2
$\sigma(\beta_\chi)$		0.4	0.2	0.5	0.3	0.3	0.4	0.3	

ment run 320 backscatter profiles were collected at each frequency. These profiles were averaged and the scattering levels calculated. Four runs were conducted to provide a mean form function and total scattering cross section with

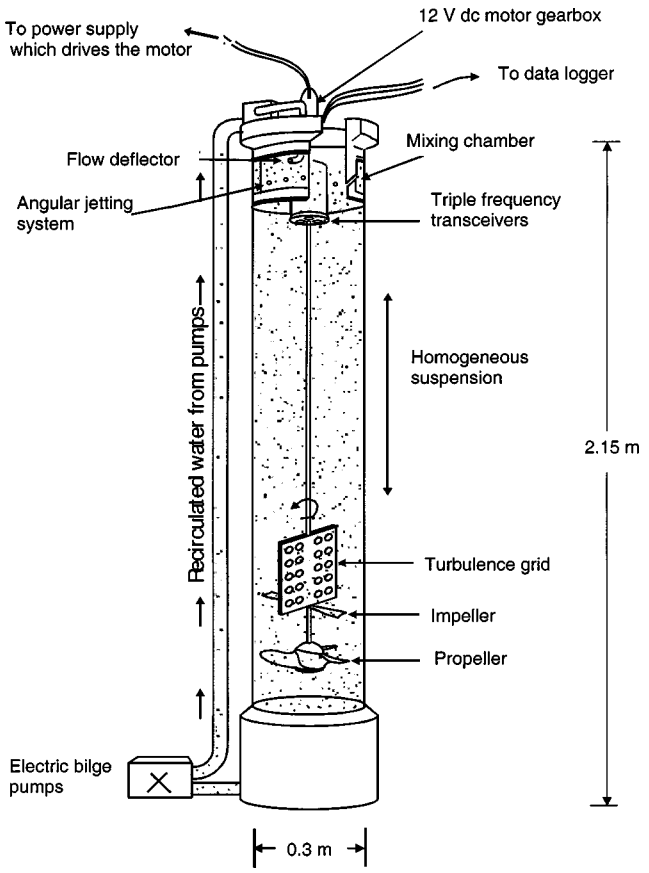

FIG. 2. The sediment tower used to measure the suspension scattering properties of glass spheres and sands.

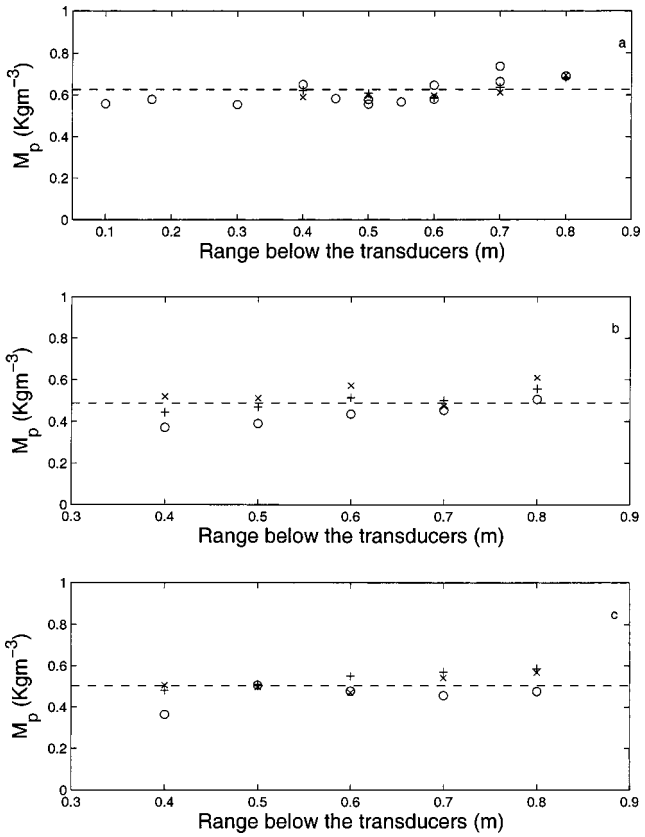

FIG. 3. Pumped sample measurements in the tower of the suspended sediment concentration with range below the transducers. Data were collected on the central axis of the tower (○), at 0.07 m from the axis (×), and at 0.14 m from the axis (+) for sediment sizes; (a) glass spheres with $\langle a_s \rangle = 115.5\ \mu$m, (b) sand with $\langle a_s \rangle = 195\ \mu$m, and (c) glass spheres with $\langle a_s \rangle = 195\ \mu$m.

error bars. This averaging was required to offset the effects of configurational noise[21] associated with the random position of the scatterers within the insonified volume and short-term fluctuations in the homogeneity of the suspension.

V. SPHERE BACKSCATTERING AND SYSTEM CALIBRATION

For all the scattering measurements, glass spheres, and sands, a common measurement procedure was adopted and this is briefly described here. After the tower had been filled with water from the mains supply, a period of several hours to days was provided, with the pumps and mixing systems running, to allow time for any bubbles present in the water to vent through the upper open water surface into the atmosphere. Acoustic backscatter data were collected over this period, and this degassing process continued until signals reduced to background levels. These varied between 1% and 10% of the levels recorded when sediment was in suspension, depending on particle size, range, frequency, and concentration. The background levels, due to detritus, residue micro-bubbles, and possibly turbulence scattering, were accounted for in the data processing procedure. Water-saturated degassed sediments were added to the tower and a period of several hours was allowed for the suspension to become homogeneous throughout the tower. Four acoustic runs were then carried out separated by approximately 5 min, with 320

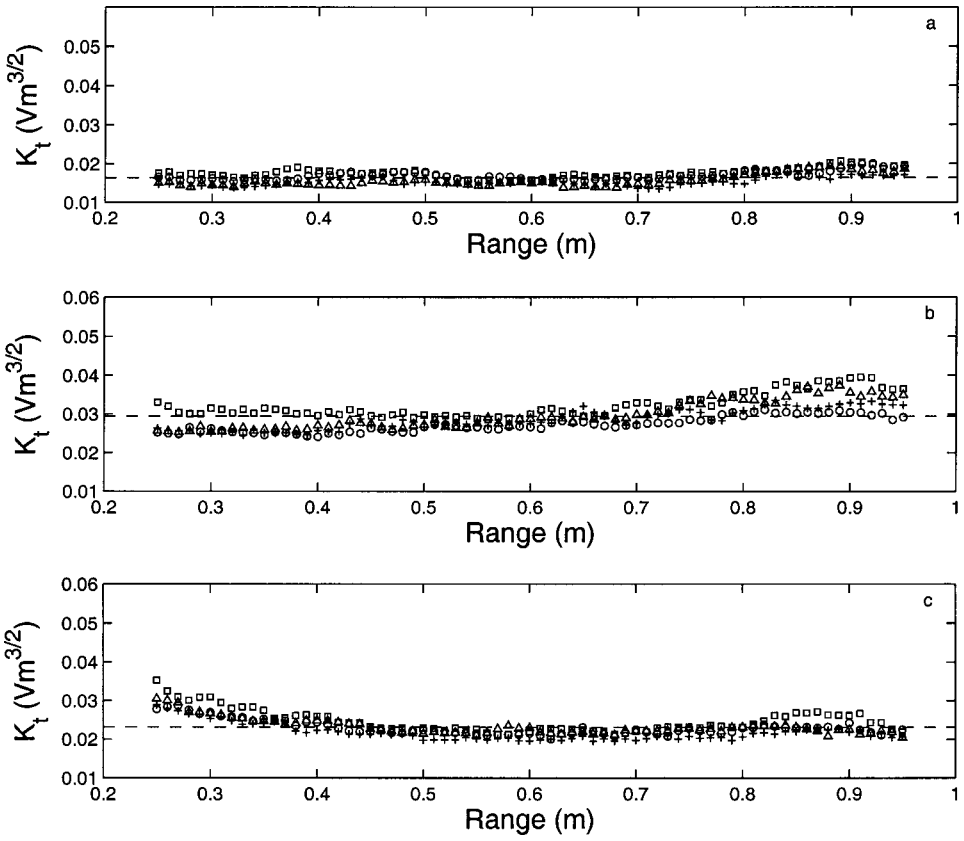

FIG. 4. Measurement of the system constant, K_t, at (a) 1.0 MHz, (b) 2.0 MHz, and (c) 4.0 MHz. The measurements were from data collected on glass spheres having mean radii of (○) 98 μm, (+) 115 μm, (△) 137 μm, and (□) 195 μm.

profiles being collected at each frequency on each run. Nominally this was repeated four times, with about 1 h between each set of four runs. At the end of the last run, pumped sampling at 0.4 and 0.75 m below the transducers was carried out to establish the concentration and homogeneity of the suspension. This series of measurements, 16 runs, constituted one experiment on one particular particle size. At the end of the experiment the sediments were extracted from the tower by placing a fine gauze net within the body of the tower. This extraction continued until acoustic background measurements showed there was no significant residue of sediment in the tower. A different sediment sample was then introduced into the tower and new acoustic and pumped sample data collected. The experiments were inter-

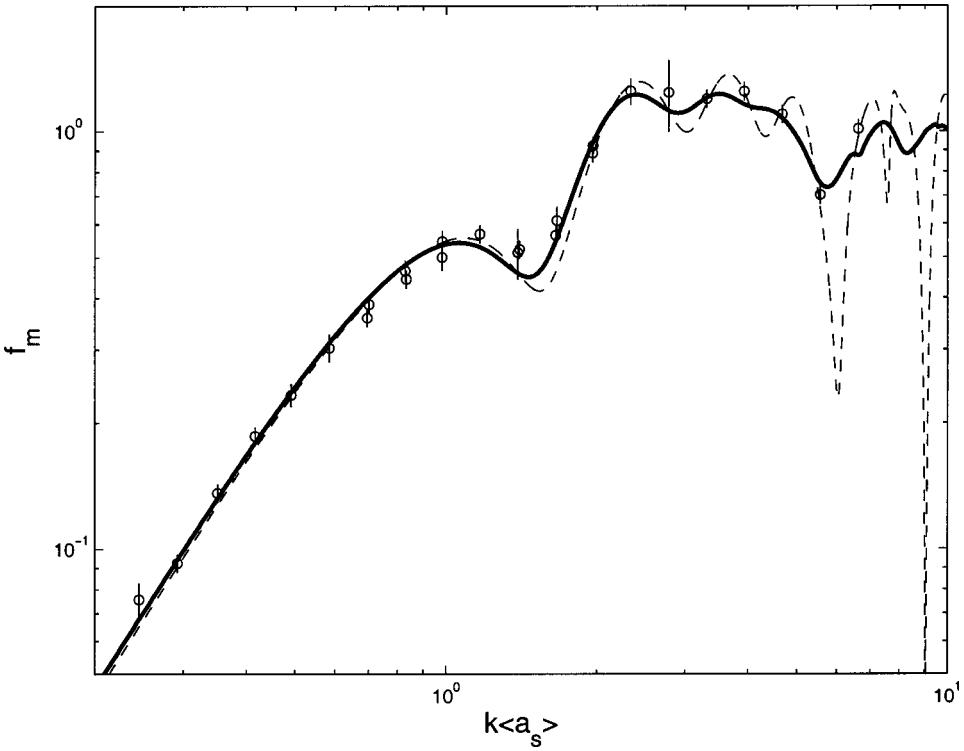

FIG. 5. Predicted and measured (○) backscatter form function for a suspension of glass spheres. The lines show the form function for the case of a single particle size in suspension (--) and for the size distribution due to the $\frac{1}{4}$ ϕ sieves used (———).

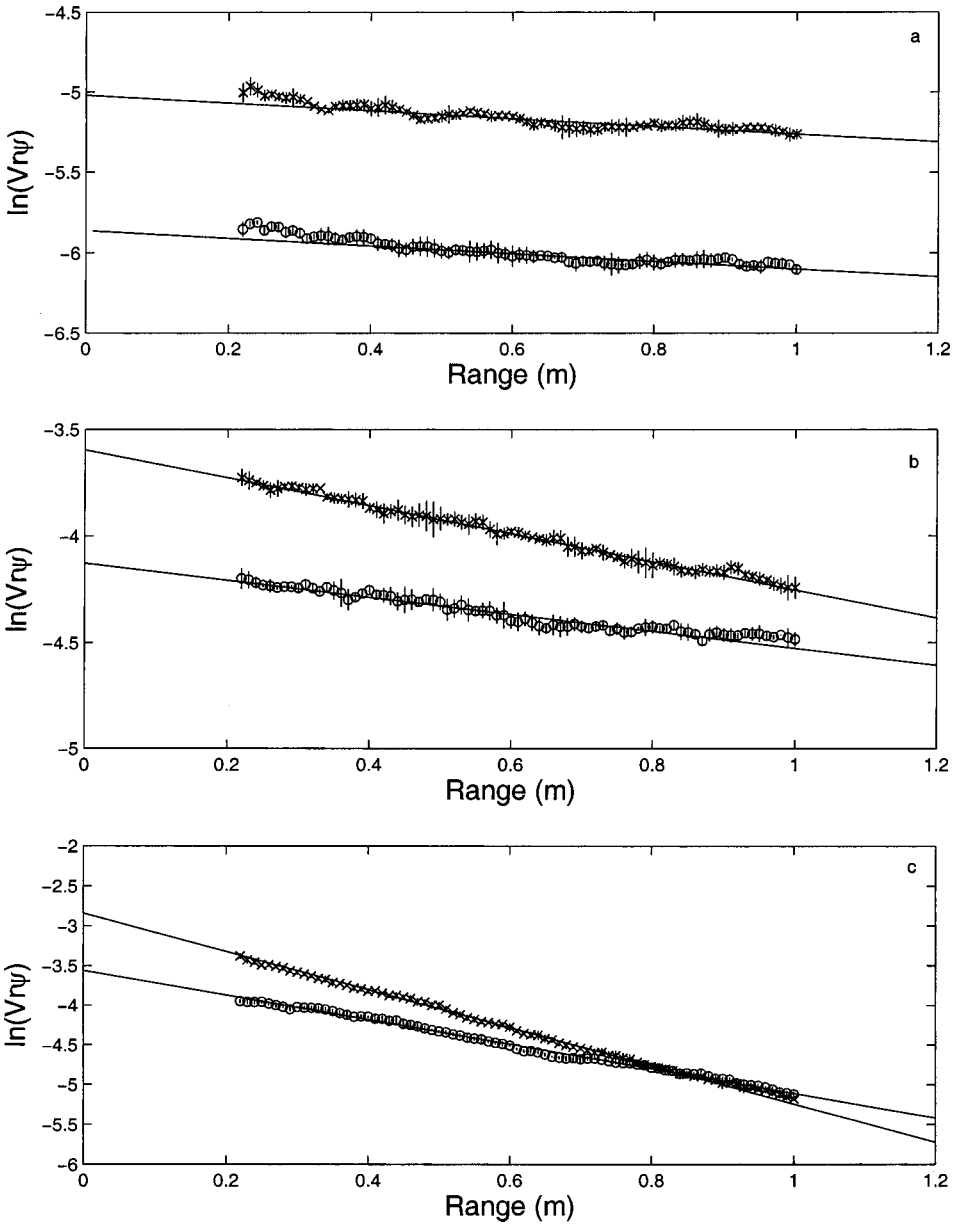

FIG. 6. Measurements of the variation of $\ln(Vr\psi)$ with range, r, from the transducer at (a) 1.0 MHz, (b) 2.0 MHz, and (c) 4.0 MHz, for sand suspensions with $\langle a_s \rangle = 57.75\ \mu$m (○) and $\langle a_s \rangle = 137.5\ \mu$m (×).

leaved with different particle sizes and repeat sizes. This procedure provided checks on the stability of the system over time and yielded error bars for the final results. The number of experiments conducted on each sediment and particle size is given in Table I.

To obtain the scattering properties of the sand suspensions required the system constant, K_t, to be known. One method is a full electronic and acoustic calibration of the system.[8,22] The electronic calibration requires measuring the voltage transfer function of the system, T_v. This includes measuring transmit signal levels, receiving amplification, and the form of the time varying gain if applied. The acoustic calibration requires measurements of the source level, $P_o r_o$, (Pa V^{-1} ref 1 m), and the receive sensitivity, $\Re$ (V Pa^{-1}), of the transducer. Also, to establish a_t generally requires the transducer beam pattern to be measured. This absolute calibration is a relatively time consuming process; however, given the sediment tower developed for the present study, most of the calibration can be circumvented by measuring the backscattered signal from suspensions with known scattering characteristics.

The calibration approach used was to rearrange Eq. (1) and have K_t on the lhs of the equation. This gives

$$K_t = \frac{Vr\psi}{K_s M^{1/2}} e^{2r\alpha}. \tag{6}$$

Conducting observations in the sediment tower on a homogeneous suspension, at a measured concentration, with a known scattering description, provided the value for the system calibration constant. Glass spheres were used for the suspension, since they were readily available in the required size range, and the scattering characteristics of glass spheres can be accurately predicted. If the electronic gain of the system is constant (this was the case for the present system), K_t has a single value; if time varying gain is applied to the system, K_t will be a function of range.

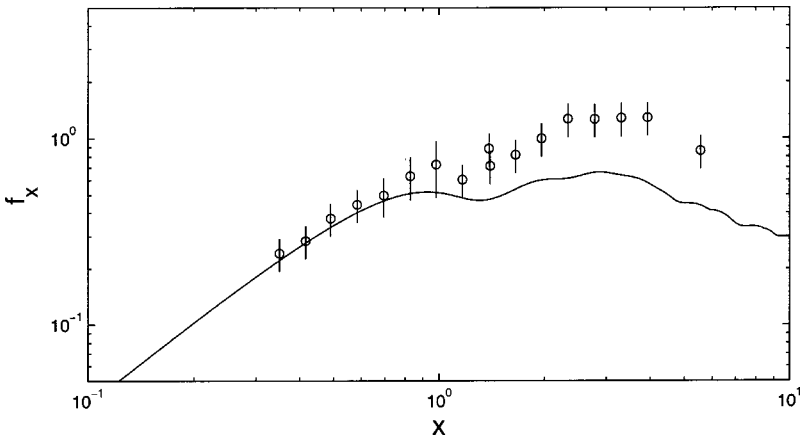

FIG. 7. Measurements of f_x (○) and calculated f_s (———) with $\gamma=1$, versus x.

An example of the measurement for K_t is given in Fig. 4. The data shown were from experiments on suspensions of glass spheres having mean radii of 98, 115, 137, and 195 μm. The plot shows the value of K_t with range for the four particle sizes. It can be seen that K_t was nominally constant with range, and the relatively small variations between the different suspensions sizes show consistent values of K_t could be obtained. The ostensibly uniform value of K_t with range further supports the homogeneity of the suspension in the tower. However, it is acknowledged that there were fluctuations in the suspension homogeneity during a run and from run to run, and this was overcome by repeating measurements and building up error statistics for the data collected.

Measurements of K_t were collected over a 3-year period interleaved with the sand suspension measurements. Carrying out glass sphere measurements at regular intervals throughout the measurement program provided an assessment of the system performance over time. To illustrate the quality of the measurements obtained in the sediment tower, the form function was calculated for the glass sphere experiments using the system constant for each frequency. The results are presented in Fig. 5. The dashed line represents the form function for a suspension having a uniform particle size; the solid line was calculated on the basis of a size distribution in suspension arising from the $\frac{1}{4}\,\phi$ sieves used to sieve the sediments. As can be seen in Fig. 5, the measured and predicted form functions show good agreement over $x=0.19-6.5$ which spans the region from the Rayleigh regime through to approximately the geometric. The error bars on the individual data are of the order of 10%–15%. It does not seem unreasonable, given the general agreement between the observations and the predictions for the glass spheres and the error bars measured, that the glass sphere observations provide an indication of the accuracy of the form function and total scattering cross section measurements for suspensions of sand grains.

VI. MEASUREMENTS ON SAND SUSPENSIONS

To obtain the form function and total scattering cross section, the expressions in Eq. (4) were employed. Examples of the data collected are shown in Fig. 6. The data show the variation of $\ln(Vr\psi)$ with range, r, from the transducer. The data were taken from two experiments carried out with sand suspensions having $\langle a_s\rangle=57.75\,\mu$m and $\langle a_s\rangle=137.5\,\mu$m. For each experiment the data have been averaged over the runs to form a mean and standard deviation. The variability observed in the data is due both to fluctuation in the suspended concentration and configuration noise. As shown in the figure, a regression line was calculated for each data set and the slope, κ, and the intercept with the ordinate, η, was measured. The first 0.2 m from the transducer were not used in the analysis to avoid the period of transmitter–receiver interference following transmission (crosstalk) and to circumvent inaccuracies in the calculation of ψ due to any imprecision in the value of a_t. Also the range was restricted to approximately 1 m to reduce signal to noise problems at the longer ranges. Using the measured value for η and κ the rhs of Eq. (4) was evaluated. It should be noted that for small values of x, nominally $x\leqslant 1$, the value for χ_x had a high degree of uncertainty due to $\kappa\approx 2\alpha_w$, therefore data analysis

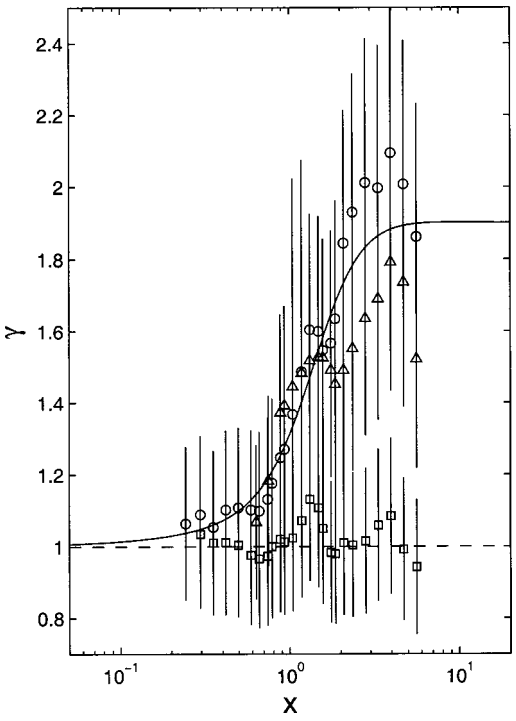

FIG. 8. Measurements for sand of the ratios f_x/f_s (○) and χ_x/χ_s (△) versus x, and Eq. (7) (———) with $\beta=1.9$. The equivalent calculation for the glass sphere results are given by (□).

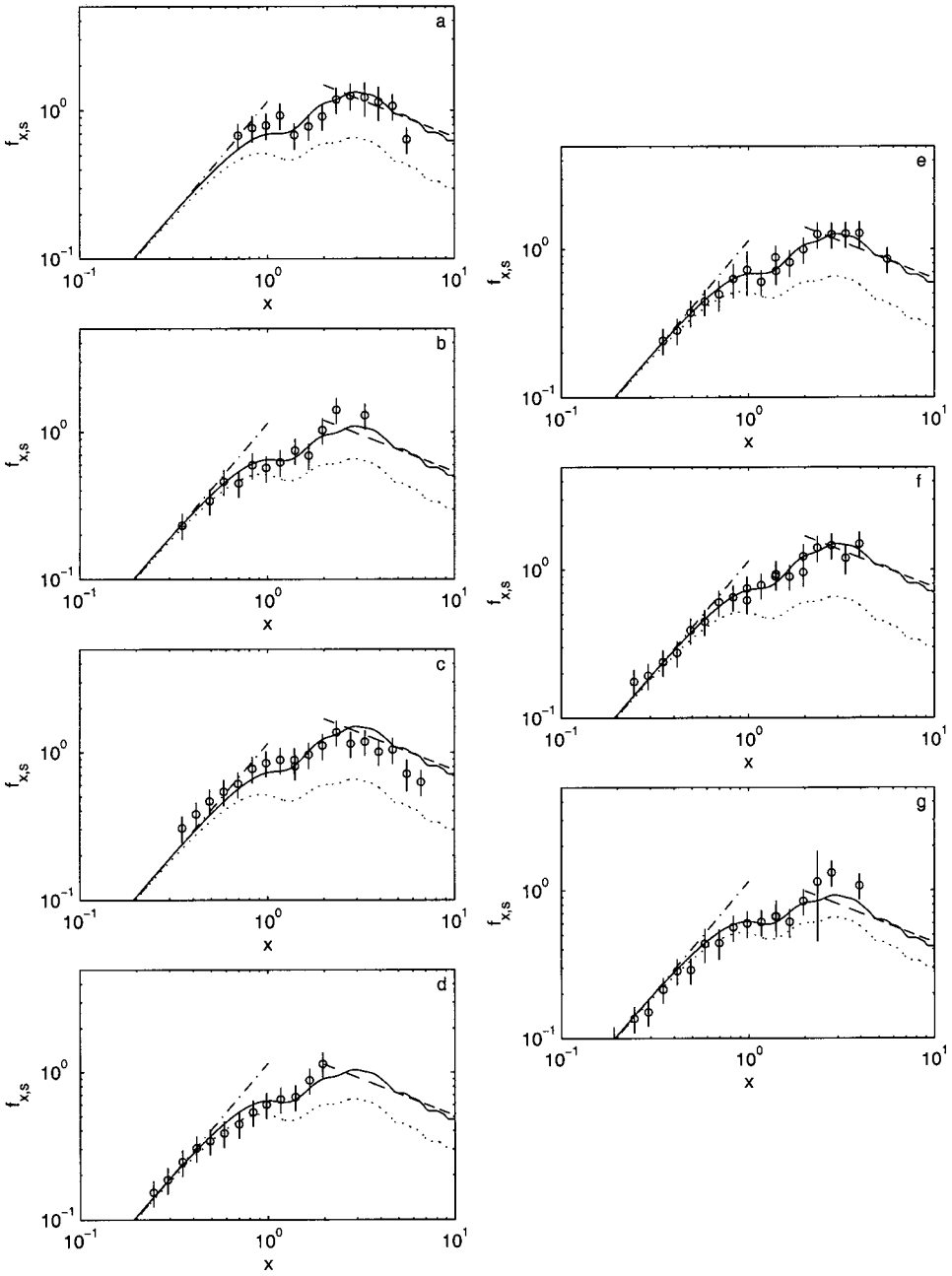

FIG. 9. Comparison of f_x (○) and f_s (———) for all of the sand suspensions, (···) $\gamma=1$ in Eq. (5a), (-·-) Rayleigh scattering and (--) geometric scattering. In the present figure and the following, plots $f_{x,s}$ represent f_x, f_s.

of the total scattering cross section was restricted to values above $x \approx 0.5$. Such a constraint did not apply to f_x.

An example of the measurements of f_x is shown in Fig. 7. The data show a steady increase in magnitude of f_x with x, with peak values in the region $x=2-3$. The solid line, f_s, was calculated using Eq. (5a) with $\gamma=1$. The measurements show that for $x \ll 1$, the Rayleigh region, the predictions based on sphere scattering are in close agreement with the observation. However, as x increases and geometric scattering is approached, there is an increased divergence between the measured value for f_x and the calculated value for f_s. Therefore, as alluded to in the Introduction, there is a functional dependence of γ on x.

To ascertain this dependence, the ratios f_x/f_s, and χ_x/χ_s, with $\gamma=1$, were calculated for all the glass sphere and sand suspension data, the outcome of which is shown in Fig. 8. Although there is scatter in the data and relatively large error bars, associated with measuring the ratios of the observed and predicted values, there is a clear trend of increasing divergence between the observations and the sphere based model with $\gamma=1$ for the sand data; however, as would be expected, no such trend is observed in the glass sphere data. To represent the difference the following simple expression was used.

$$\gamma = \frac{\beta x^3 + 0.5x + 3.5}{x^3 + 3.5}. \tag{7}$$

This had the required form, reducing to unity in the Rayleigh regime, increasing over the intermediate values for x, remaining constant for geometric scattering and with β accounting for the enhance scattering in the geometric regime. The structure of this curve is shown in Fig. 8 with $\beta=1.9$. β is the free parameter; it is independent of x and represents the

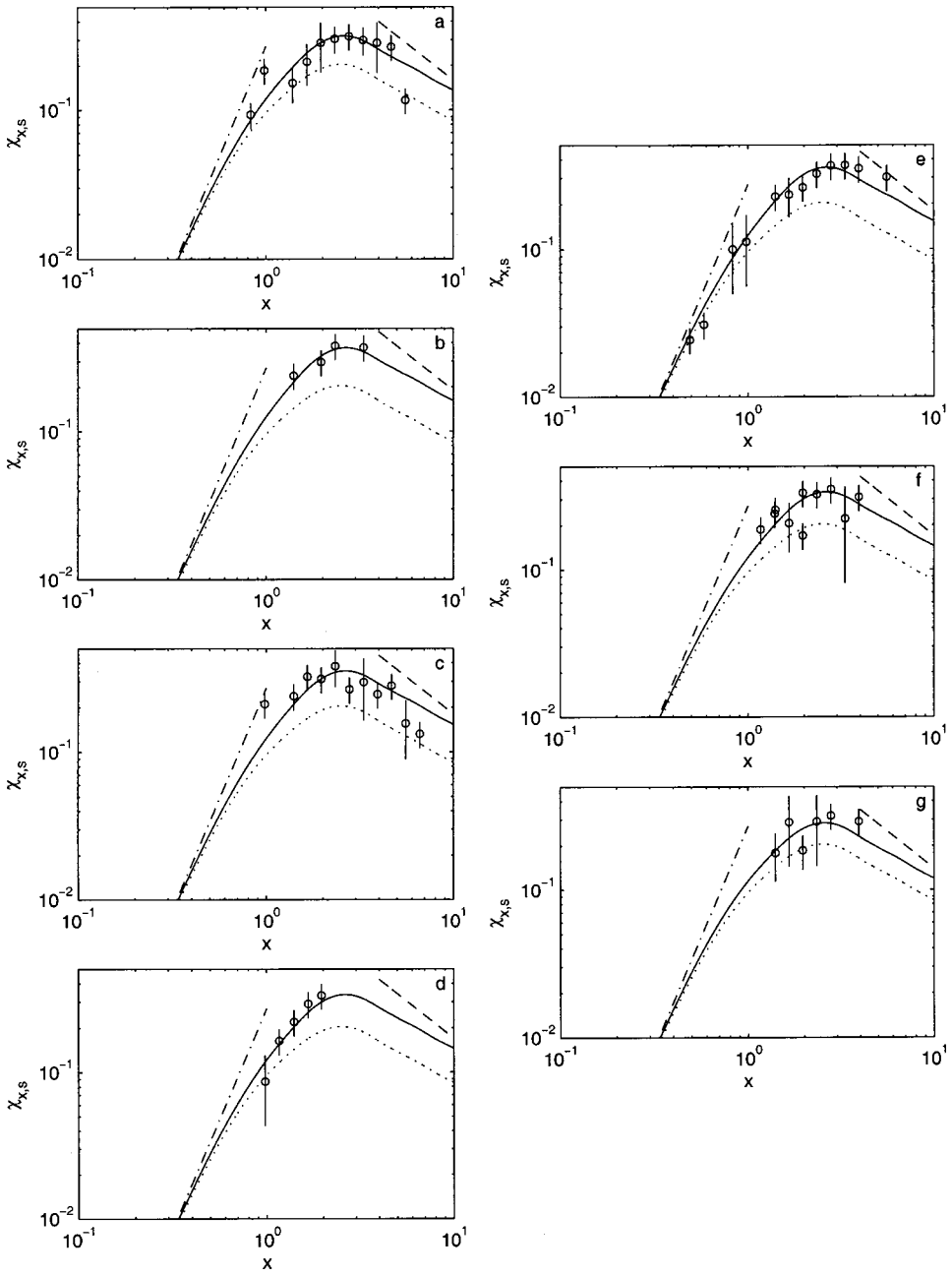

FIG. 10. Comparison of χ_x (○) and χ_s (———) for all of the sand suspensions, (···) $\gamma=1$ in Eq. (5b), (-·-) Rayleigh scattering and (--) geometric scattering. In the present figure and the following, plots $\chi_{x,s}$ represents χ_x, χ_s.

upper limit of γ. Equation (7) can be seen to compare reasonably well the data and, to first order, represents the enhanced scattering for irregularly shaped particles, from the Rayleigh regime through to the geometric scattering regime.

For comparison of the sphere model with the individual sediments used in the study, the value for β was allowed to vary and no constraint was placed on using the same value of β for calculating f_s and χ_s. To obtain the optimum value for β a routine was used which minimized $|\Gamma_x-\Gamma_s|/\Gamma_s$, where Γ was f or χ, as β was varied between 0.5 and 2.5 in step intervals of 0.1. The resulting values of β with calculated standard deviations are given in Table I. The results for the backscattering cross section measurements are shown in Fig. 9. The plots show the measured values for f_x, the low pass sphere calculations f_s using γ with β values from Table I, f_s with $\gamma=1$ and Rayleigh and geometric scattering. In general it can be seen that the enhanced sphere model reproduces the general features of the data. There is initially an increase in f_x and f_s with a $x^{3/2}$ dependency in the low x region. This is followed by a reduction in the increase of f_x and f_s, with a maximum value at $x\approx 3$. At higher values of x, as the geometric region is approached, there is a reduction of f_x and f_s which approaches a $x^{-1/2}$ dependency on x. There are minor divergences from these trends and there is some scatter in the data, both of which are probably associated with the detailed mineralogy, particle shape, and experimental uncertainty. However, as can be seen, the expression for γ does provide a reasonably accurate correction factor to the sphere scattering model. Figure 10 compares χ_x and χ_s. The measurement region is limited to $x>0.5$ for reasons previously outlined and the data is somewhat more variable than the measurement of the backscattering cross section. Within the limitation of the data set collected, the observation of χ_x and the calculated values for χ_s are in broad agreement.

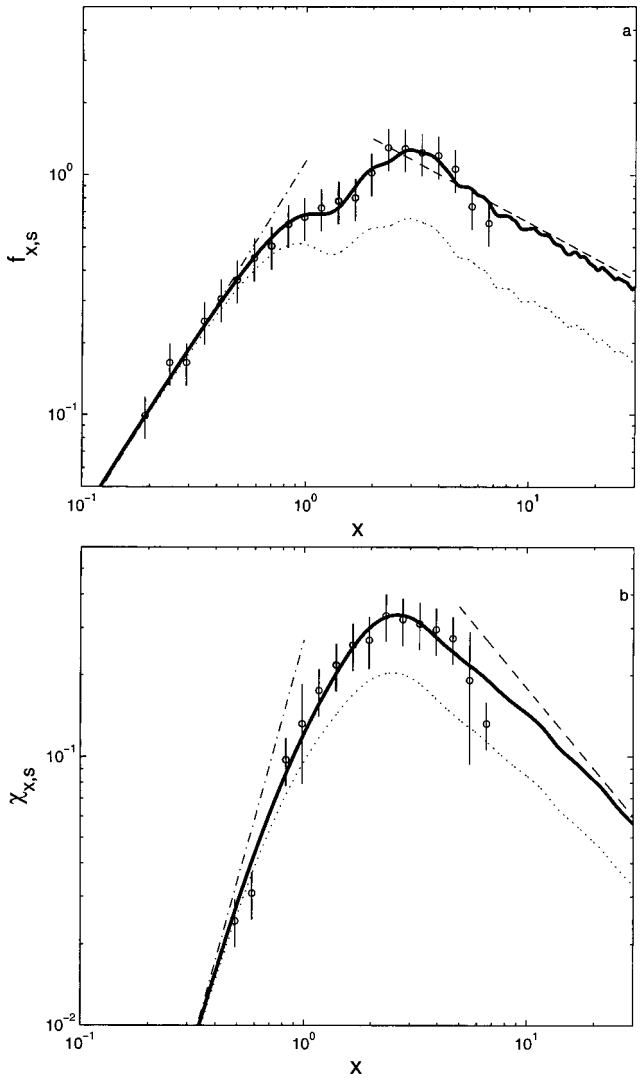

FIG. 11. (a) The variation in f_x (○) obtained by combining all the measurement on sand suspensions. (———) f_s with $\beta=1.9$, (···) f_s with $\gamma=1$. (b) The variation in χ_x (○) obtained by combining all the measurement on sand suspensions. (———) χ_s with $\beta=1.7$, (···) χ_s with $\gamma=1$. (-·-) is Rayleigh scattering and (--) is geometric scattering.

There is a reduction in χ_x and χ_s for low values of x, although only limited reliable observations could be obtained in the Rayleigh region to assess the x^3 dependency, the peak in the observations and calculation is around $x\approx 2.6$, and there is a reduction in χ_x and χ_s with x above this value, though it is difficult to fully validate the geometric x^{-1} dependency due to the upper limit of x in the data set.

In Fig. 11 all the sand suspension data have been combined to give representative values for f_x and χ_x. Figure 11(a) shows the variation of f_x and it can be seen the data follow the Rayleigh dependency for $x \ll 1$ and approach the geometric value for $x \gg 1$, though the data are marginally lower at the highest values of x measured. However, it is difficult to assess if this lower trend is genuine because of the upper limit of x measured. The form of f_s with $\beta=1.9$, given by the broad line, is in good agreement with the data and represents reasonably well the observations. The dotted line represents the sphere calculation with $\gamma=1$. Figure 11(b) shows the measurement for χ_x. Averaging the data over the seven different sand suspensions helps to clarify the tend in the measurements. Comparison of χ_s with $\beta=1.7$, shown by the broad line, shows acceptable agreement with the data over the limited range of x for which reliable values of χ_x could be measured. Again the dotted line shows the result when $\gamma=1$.

The data in Figs. 9–11 broadly support the low pass sphere, γ enhanced, description based on a single variable β. To further assess the general applicability of the γ term, previously reported data sets were examined. The first of these to be assessed was measurements[5] of the total scattering cross section collected on suspensions of sands. The data set complements the present study, in that a broad frequency range, nominally 1–100 MHz, was used on a limited number of sediment sizes, as opposed to the present work where a relatively narrow frequency band, 1–4 MHz, was used with a broad range of sediments and sediment sizes. In the analysis presented in Ref. 5 the data was fitted to a movable rigid sphere model, formulated using a two-parameter approach, to rescale χ_x on the ordinate and x on the abscissa. Inspection of the data, before rescaling, shows very similar trends to those of the present data; with low x values having approximately Rayleigh scattering, followed by increased enhanced scattering relative to a sphere as x increased, remaining at an almost constant difference in the geometric region. It was therefore considered interesting to compare how well the γ term of Eq. (7) accounted for the difference in the low pass sphere model and sediment scattering in this data set. Figure 12 shows a comparison of the γ enhance sphere scattering model, Eq. (5b), with the data. For the comparison, the value used for $\langle a_s \rangle$ was obtained from the sieved sizes given in the paper and not the optical diffraction size used by the authors in their analysis. The sieved size was chosen to be consistent with the present study. Therefore the abscissa was rescaled for x values based on the sieved size. For the quartz sediment no sieve size was available and therefore the optical diffraction size was scaled to a sieve size based on the other sediments where both measurements had been obtained. Table II lists the sediments and the values for $\langle a_s \rangle$. It can readily be seen in the plots that the application of the γ term does bring the low pass sphere model into close agreement with the measurements and accounts for most of the difference between the sphere and sediment scattering. The range of β, presented in Table II, between 1.2 and 2.2 is comparable with the values given in Table I. It is seen from Table II that β_χ increases with decreasing particle size. As noted in Ref. 5, this is considered to be associated with greater irregularity in the particle shape with reducing size. This increases the surface area relative to a sphere of nominally the same size and hence increases the geometric scattering cross section leading to higher values of β_χ. The results from the present study and those of Fig. 12 are therefore essentially equivalent in terms of the physical interpretation of the enhanced scattering with x.

The final comparison conducted is with the original data of Hay[2] which provided the first measurements of the form function for suspensions of sand grains. A relatively complicated jetting system was used to generate the suspension and measurements were conducted at 1, 2.25, and 5 MHz. The

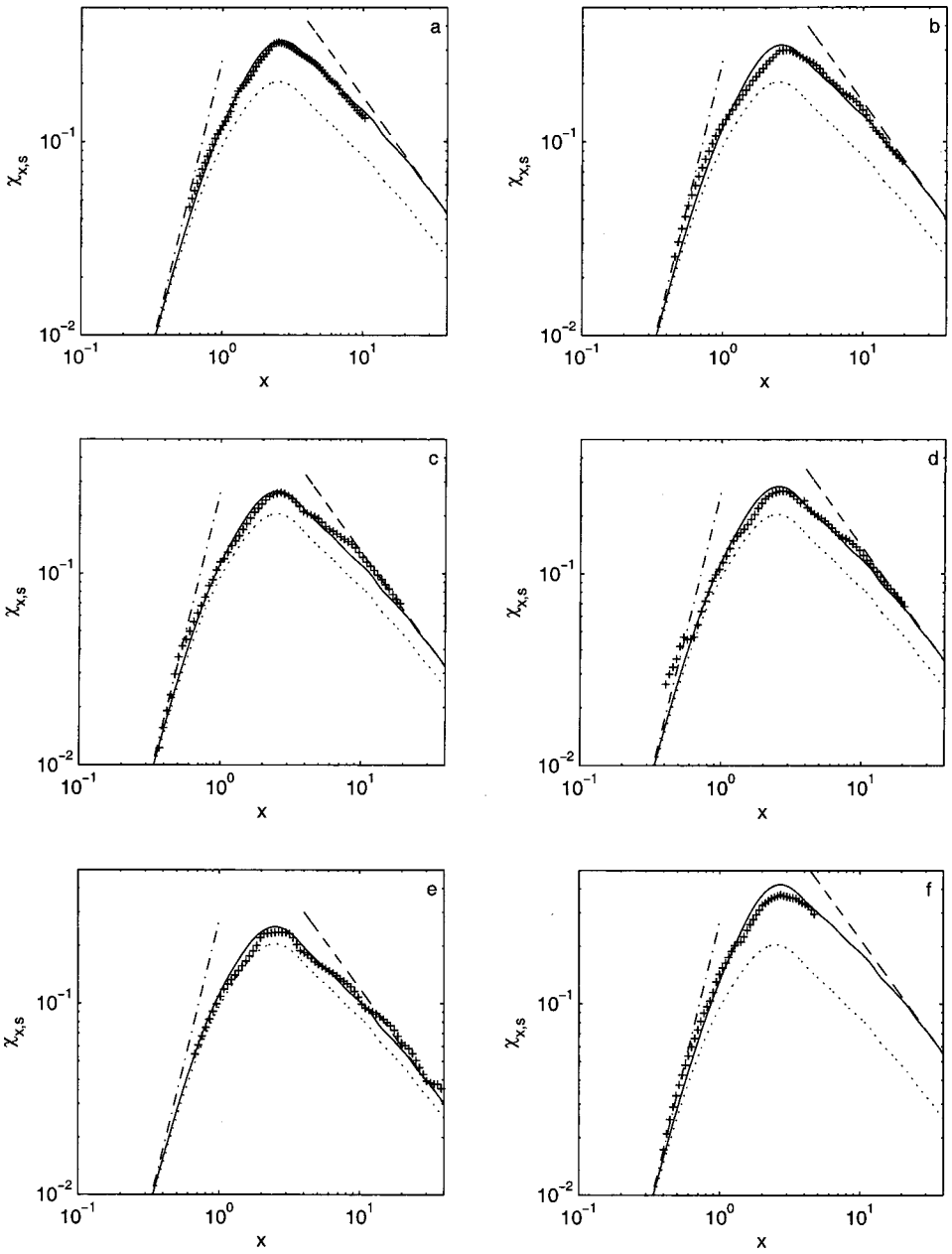

FIG. 12. Comparison of χ_x (+) and χ_s (———) for the sand suspensions of Ref. 5, (···) $\gamma=1$ in Eq. (5b), (-·-) Rayleigh scattering and (--) geometric scattering. (a) Assen sand 1, (b) Assen sand 2, (c) Ottawa sand, (d) Twente sand, (e) dune sand and (f) quartz particles.

results are presented in Fig. 13. Relative to the sphere scattering curve with $\gamma=1$, there is enhanced scattering. There is Rayleigh type behavior at low values of x, although the values appear somewhat elevated, between $x=1$ and 3 there is increasing divergence from the sphere scattering model with $\gamma=1$, while above $x=3$, the degree of elevation is variable. Applying the γ term does improve agreement with the data, although due to the small value of β_f, $\beta_f=1.2$, the effect is not as notable as in Fig. 9. Although this value is below the values observed in the present study, there is variability in β_f and this may simply be associated with this. Otherwise, at present, the difference in β_f between the present data set in Fig. 9, and Ref. 2 in Fig. 13, is not readily explainable.

TABLE II. The sediments used in Ref. 5. The second row gives the value for $\langle a_s \rangle$ in micrometers obtained from sieving, apart from the quartz particle which was estimated (see text). The third row gives the values of β_χ used in Eq. (7).

Assen 1	Assen 2	Ottawa	Twente	Dune	Quartz
24.5	49	49	49	98	11.5
1.7±0.1	1.6±0.1	1.3±0.1	1.4±0.1	1.2±0.1	2.2±0.2

VII. DISCUSSIONS AND CONCLUSIONS

The present study focused on examining the scattering properties of suspensions of marine sands. The work is part of on-going studies into the application of acoustics to the measurement of sediment processes. To obtain particle size and concentration, from the signal backscattered from a suspension of sediments, requires knowledge of the scattering properties of the sediments, which are used in an inversion algorithm to obtain sediment parameters. Here we have presented a series of measurements on different sands, broadly covering the Rayleigh, intermediate, and geometric scattering regimes. The model used to examine the data was that of

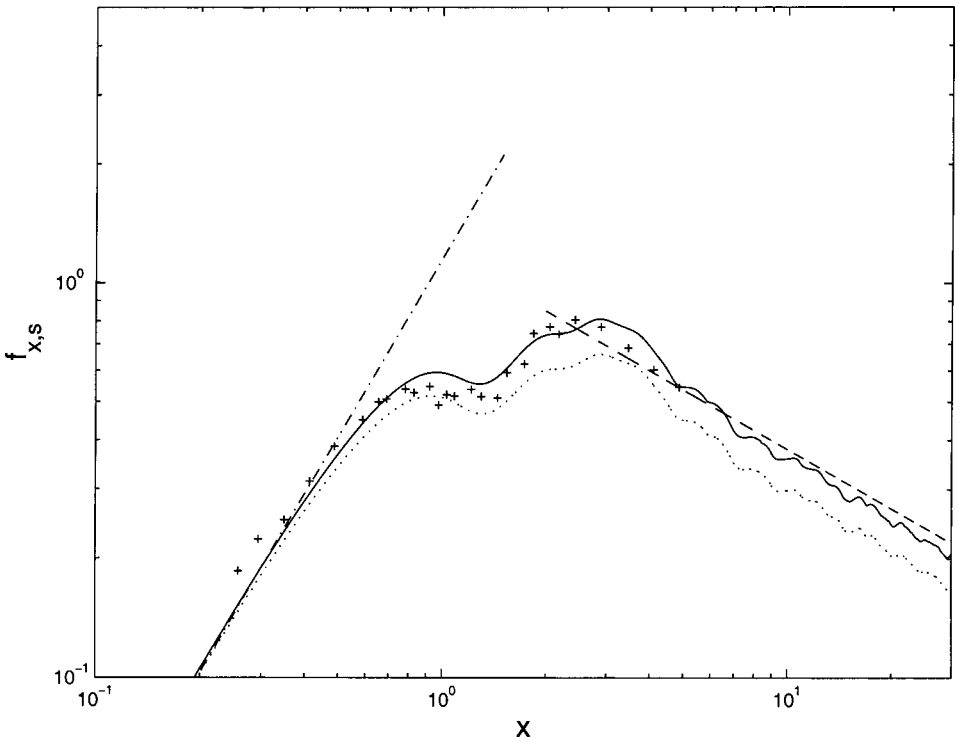

FIG. 13. Comparison of f_x (+) and f_s (———) for the sand suspensions of Ref. 2, (···) $\gamma=1$ in Eq. (5a), (-·-) Rayleigh scattering and (--) geometric scattering.

an elastic sphere modified using a smoothing function to remove the rapid oscillation normally observed in the form function for a sphere. The comparison showed that at low values of x, within the Rayleigh scattering regime, the scattering of sand grains is comparable with that of a sphere of similar size as measured by standard sieving. Above the Rayleigh region, there is a divergence between the sphere model and the observed scattering characteristics of sand, and this divergence is enhanced with increasing x up to $x\approx 3$. At higher values of x, as the geometric scattering region is approached, the difference in the sand and sphere scattering remains constant. The latter has been interpreted in terms of a theorem which states that the geometric cross section of a convex particle, averaged over all orientations, is equal to a quarter of the surface area of the particle. At high frequencies it is the geometric cross section which is measured and hence elevated scattering relative to a sphere would be expected. To account for the difference between the sphere model and the sediment scattering characteristics an enhancement factor, the γ term, was introduced. This term accounted for most of the differences between sphere model and the data collected for the present study. Application of the approach to other data sets gave similar improved agreement. Therefore, to first order, the γ term appears to have general applicability for sand suspensions. It has only one free parameter, β, which primarily rescales the γ term in the geometric region and thereby provides a simple relationship between the sphere model and the measured scattering characteristics of suspensions of sand.

In Ref. 5 a qualitative attempt was made to related particle shape irregularity, obtained from visual inspection of scanning electron micrographs, to their rescaling parameters. Although the approach was subjective, there did appear to be some correlation between particle size, estimated irregularity, and their rescaling parameters. In the present study the collected data was replotted, with $\langle a_s \rangle$ as the abscissa variable, to examine if there was any relationship between particle size and β; however, none was observed. Also visual inspection of the particle shapes in the scanning electron micrographs in Fig. 1, does not show an obvious relationship with the β values give in Table I. For each sediment examined, a number of sieved size fractions were used to obtain a range of $k\langle a_s \rangle$, and it may be that these had somewhat different shapes, which might have weakened any simple obvious relationship between the micrograph images for a particular sediment and the value of β. It may also be the case that simple visual inspection of scanning electron micrographs is not a sufficient parametrization of the particles and a more quantitative approach is required.

The reasons for conducting the present work are both ones of interest in the scattering problem and of making a contribution to the application of acoustics to sediment transport processes. For the sedimentologist their requirement is to use acoustics as a tool. It is clear from this study and that of Ref. 5 that individual sediments have somewhat different scattering characteristic depending on precise shape and composition. Unfortunately, this variability is not insignificant, and needs to be accounted for when extracting suspended sediment parameters from backscatter data. Although Ref. 5 showed increasing β_χ with reducing particle size, due to shape, the present data show β_f and β_χ for the larger particle sizes having comparable values to the smaller particles analyzed in Ref. 5. Therefore one could consider consolidating all the measurements of β reported here. Doing so gave $\beta_f=1.8\pm0.4$ and $\beta_\chi=1.6\pm0.3$. Further, since the mean values for β_f and β_χ are not significantly different when account is taken of the standard deviations, the data for β_f and β_χ could be combined to give $\beta=1.7\pm0.3$. Since, to first order, the γ term provides a generic description of the enhanced sand scattering relative to a sphere, this can be

utilized for inverting acoustic backscatter data to sediment concentration and particle size. There is one free parameter β, which is variable for different sediments and account needs to be taken of this variability, to provide error estimates for the sediment parameters extracted from the acoustic inversion.

ACKNOWLEDGMENTS

The authors would like to thank James Ellis, Judith Wong, Mairead Butler, and Kyle Betteridge for their contributions to the collection of the data. This paper was begun during a visit by PDT to the Marine Physical Laboratory at Scripps USA in March–April of 2003. PDT would like to thank Professor Michael J Buckingham for the invitation to work at Scripps and for the stimulating and interesting time he had. The work was funded by NERC, UK and ONR under its mine burial program.

[1] P. D. Thorne and D. M. Hanes, ''A review of acoustic measurement of small-scale sediment processes,'' Cont. Shelf Res. **22**, 603–632 (2002).
[2] A. E. Hay, ''Sound scattering from a particle-laden turbulent jet,'' J. Acoust. Soc. Am. **90**, 2055–2074 (1991).
[3] H. Cheng and A. E. Hay, ''Broadband measurements of the acoustic backscatter cross section of sand particles in suspension,'' J. Acoust. Soc. Am. **94**, 2247–2254 (1993).
[4] P. D. Thorne, K. R. Waters, and T. J. Brudner, ''Acoustic measurements of scattering by objects of irregular shape,'' J. Acoust. Soc. Am. **97**, 242–251 (1995).
[5] A. S. Schaafsma and A. E. Hay, ''Attenuation in suspensions of irregularly shaped sediment particles: A two-parameter equivalent spherical scatterer model,'' J. Acoust. Soc. Am. **102**, 1485–1502 (1997).
[6] J. Sheng and A. E. Hay, ''An examination of the spherical scatterer approximation in aqueous suspensions of sand,'' J. Acoust. Soc. Am. **83**, 598–610 (1988).
[7] G. H. Flammers, ''Ultrasonic measurements of suspended sediments,'' Geo. Survey Bull. No. 1141-A. (US GPO, Washington, DC, 1962).
[8] P. D. Thorne, P. J. Hardcastle, and R. L. Soulsby, ''Analysis of acoustic measurements of suspended sediments,'' J. Geophys. Res. **98(C1)**, 899–910 (1993).
[9] T. K. Stanton, D. Chu, P. H. Wiebe, and C. S. Clay, ''Average echoes from randomly orientated random-length finite cylinders: Zooplankton models,'' J. Acoust. Soc. Am. **94**, 3463–3472 (1993).
[10] T. K. Stanton, D. Chu, and P. H. Wiebe, ''Sound scattering by several sound zooplankton groups. II. Scattering models,'' J. Acoust. Soc. Am. **103**, 236–253 (1998).
[11] T. K. Stanton and D. Chu, ''Review and recommendations for modeling of acoustic scattering of fluid-like elongated zooplankton: Euphausiids and copepods,'' ICES J. Mar. Sci. **57**, 793–807 (2000).
[12] J. W. S. Rayleigh, *The Theory of Sound* (Dover, New York, 1945), Vol. II, p. 504.
[13] D. R. Palmer, ''Rayleigh scattering from nonspherical particles,'' J. Acoust. Soc. Am. **99**, 1901–1912 (1996).
[14] H. C. van de Hulst, *Light Scattering by Small Particles* (Dover, New York, 1981), p. 470.
[15] P. A. Chinnery, V. F. Humphrey, and J. Zhang, ''Low-frequency acoustic scattering by a cube. Experimental measurements and theoretical predictions,'' J. Acoust. Soc. Am. **101**, 2571–2582 (1997).
[16] A. Downing, P. D. Thorne, and C. E. Vincent, ''Backscattering from a suspension in the nearfield of a piston transducer,'' J. Acoust. Soc. Am. **97**, 1614–1620 (1995).
[17] G. C. Gaunaurd and H. Uberall, ''RST analysis of monostatic and bistatic acoustic echoes from an elastic sphere,'' J. Acoust. Soc. Am. **73**, 1–12 (1983).
[18] P. D. Thorne and S. C. Campbell, ''Backscattering by a suspension of spheres,'' J. Acoust. Soc. Am. **92**, 978–986 (1992).
[19] P. D. Thorne, L. Hayhurst, and V. F. Humphery, ''Scattering by nonmetallic spheres,'' Ultrasonics **30**, 15–20 (1992).
[20] G. W. C. Kaye and T. H. Laby, *Tables of Physical and Chemical Constants* (Longman, New York, 1973), p. 477.
[21] C. Libicki, K. W. Bedford, and J. F. Lynch, ''The interpretation and evaluation of a 3-MHz acoustic backscatter device for measuring benthic boundary layer sediment dynamics,'' J. Acoust. Soc. Am. , 1501–1511 (1989).
[22] P. D. Thorne and P. J. Hardcastle, ''Acoustic measurements of suspended sediments in turbulent currents and comparison with *in situ* samples,'' J. Acoust. Soc. Am. **101**, 2603–2614 (1997).